Computational Image Processing of Ovarian Cancer Cells in Varying Mechanical Environments

Nuran Golbasi, Mustafa Kemal Ruhi, Zachary Young, Linda Henry, Margaret Elizabeth Stanley, Dr. Imran Rizvi, Dr. William Polacheck

Joint Department of BIOMEDICAL ENGINEERING
UNC LINEBERGER COMPREHENSIVE CANCER CENTER
UNC CHAPEL HILL
NC STATE UNIVERSITY

INTRODUCTION

Ovarian Cancer

- Although ovarian cancer is only the 17th most common cancer, it is the leading cause of gynecologic cancer-related death[1].
- Has poor prognosis due to late diagnosis, chemoresistance, metastasis, and recurrence[2,3].
- Tumors primarily metastasize along ascitic currents in the peritoneal cavity[3].

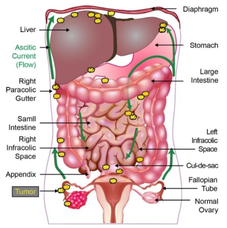

Figure 1. Ovarian Cancer Metastases with tumor cells in yellow and ascitic currents in green (Nath et al., 2020).

Tumor Microenvironment

- A significant determinant of tumor behavior, the tumor microenvironment (TME) is characterized by cellular and noncellular components as well as various mechanical stresses, including interstitial fluid pressure, solid stress, and flow-induced shear stress[2, 5].

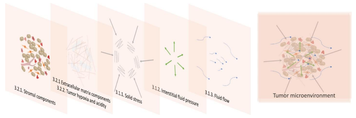

Figure 2. Tumor microenvironment and its components: stromal, extracellular matrix, solid stress, interstitial fluid pressure, fluid flow (Sorrin et al., 2020).

- The TME has elevated interstitial fluid flow, which can affect cell migration through mechano-transduction[6].
- Mechano-transduction regulates cellular responses to the microenvironment as mechanical forces can drive signaling, function, cell adhesion, and proliferation[7].
- Both substrate stiffness and flow can mimic the mechanical microenvironment and modulate cell shape, adhesion and spreading[4,7].

Marker-Controlled Watershed Segmentation

- The watershed segmentation technique is an established algorithm for image segmentation.
- It is derived from the topographical concept of a watershed and separates an image into catchment basins[8].
- The algorithm calculates watershed lines of a grayscale image, producing a label matrix[8].
- Pixel values of 0 correspond to watershed lines, while pixel values of 1+ correspond to catchment basins[8].

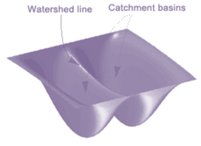

Figure 3. Watershed Catchment Basin (MathWorks, 2020).

WORKFLOW & RESULTS

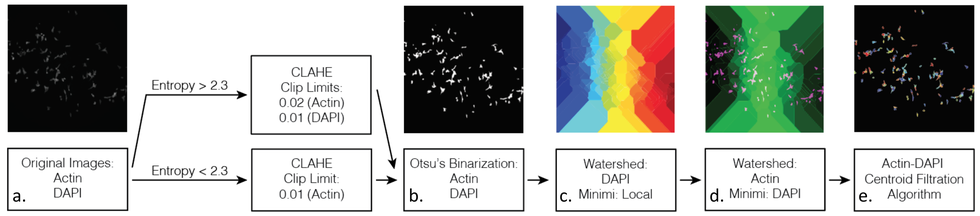

Figure 6. Substrate Stiffness Image Set (a) Original image was classified after thresholding according to its entropy. (b) Phalloidin (actin) and Dapi (nuclei) channels were equalized with different clip limits through a contrast-limited adaptive histogram equalization according to entropy classification. (c) Binarization of actin and nuclei through Otsu's method. (d) Marker-controlled watershed transform of nuclei by imposing local minima on a distance transform of the binarization. (e) Marker-controlled watershed transform of actin by imposing nuclei on a gradient of the grayscale actin image. (f) Actin removed through filtration algorithm if it did not contain the centroid of a nucleus.

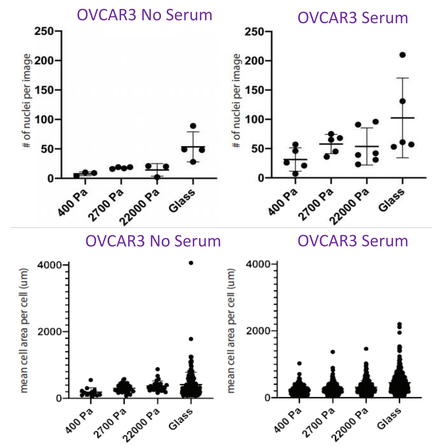

Figure 7. Cell count of OVCAR-3 cells on PA gels increases in the presence of serum due to increased adhesion. However, the cell area of OVCAR-3 cells is unaffected by the presence of serum.

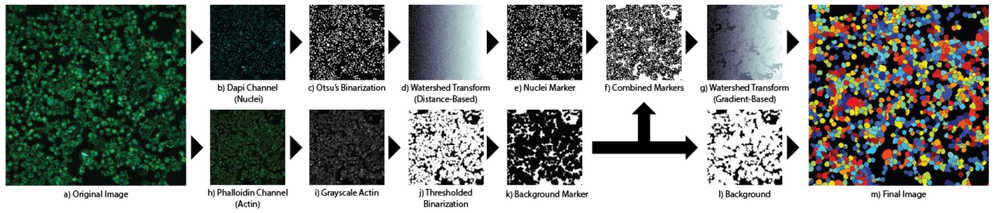

Figure 8. Flow-Induced Shear Stress Image Set (a) Original image of cell with both channels. (b) Dapi channel corresponding to the nuclei of cells. (c) Binarization of nuclei through Otsu's method after one application of contrast-limited adaptive histogram equalization. (d) Marker-controlled watershed transform of nuclei by imposing local minima on a distance transform of the binarization to produce a label matrix. (e) Label matrix applied to binarized image to produce nuclei markers. (f) Phalloidin channel corresponding to the actin in the cell. (g) Grayscale image of the actin. (h) Binarization of actin with manual thresholding; threshold derived from histograms of pixel intensity of the grayscale image of actin. (i) Inverted image of actin with smaller regions removed to produce background markers. (j) Marker-controlled watershed transform of actin by imposing nuclei and background markers on the gradient of the grayscale image of actin to produce final segmented image of actin with centroids labeled as dots.

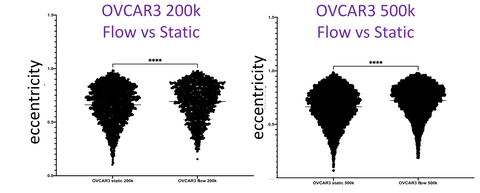

Figure 7. Cell area of OVCAR-3 cells under flow is higher than cell area under static conditions at both 200k and 500k density. Eccentricity of OVCAR-3 cells under flow is also higher than cell area under static conditions at both 200k and 500k density.

METHODS

Substrate Stiffness Image Set

- OVCAR3 cells and ES2 cells on PA gels (400 – 22,000 PA) and glass coated with fibronectin or collagen in the presence and absence of serum
- Watershed Segmentation Technique using distance transform of binary images and imposing local minima as nuclei to diminish over-segmentation

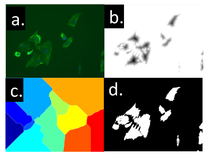

Figure 4.
a. Original actin
b. Distance Transform
c. Watershed Transform
d. Split actin

Flow-Induced Shear Stress Image Set

- OVCAR3 and CaOV3 cells in perfusion models under flow and static conditions at various cell densities (100k-500k)
- Watershed segmentation technique adjusted due to the challenge of binarizing high cell density images.
- Input is the gradient of grayscale actin with both background and foreground (nuclei) markers imposed as minima.

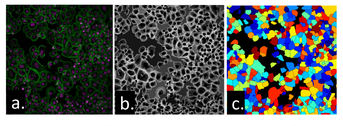

Figure 5. (a) Original actin with nuclei. (b) Gradient of grayscale actin. (c) Final segmented actin.

CONCLUSION

- Through a novel application of the marker-controlled watershed segmentation technique, we developed a workflow to analyze images of cells under various conditions and derived phenotypic metrics.
- Not only did this method quantify visible trends such as increases in cell area, but it also captured metrics, such as major axis length and orientation, that could not have been found otherwise.
- Our analysis showed us that flow-induced shear stress increases cell area and eccentricity in perfusion models at high densities, while the presence of serum on PA gels did not affect cell area.
- These metrics can provide important insights into molecular mechanisms and mechano-transduction to inform improved treatments for ovarian cancer.
- This workflow can be adjusted and applied to a variety of cell images for future development.

REFERENCES

1. *Cancer of the Ovary—Cancer Stat Facts*. (n.d.). SEER. Retrieved April 29, 2021, from https://seer.cancer.gov/statfacts/html/ovary.html
2. Chien, J., Kuang, R., Landen, C., & Shridhar, V. (2013). Platinum-Sensitive Recurrence in Ovarian Cancer: The Role of Tumor Microenvironment. *Frontiers in Oncology*, *3*. https://doi.org/10.3389/fonc.2013.00251
3. Rizvi, I., Gurkan, U. A., Tasoglu, S., Alagic, N., Celli, J. P., Mensah, L. B., Mai, Z., Demirci, U., & Hasan, T. (2013). Flow induces epithelial-mesenchymal transition, cellular heterogeneity and biomarker modulation in 3D ovarian cancer nodules. *Proceedings of the National Academy of Sciences of the United States of America*, *110*(22), E1974-1983. https://doi.org/10.1073/pnas.1216989110
4. Nath, S., Pigula, M., Khan, A. P., Hanna, W., Ruhi, M. K., Dehkordy, F. M., Pushpavanam, K., Rege, K., Moore, K., Tsujita, Y., Conrad, C., Inci, F., del Carmen, M. G., Franco, W., Celli, J. P., Demirci, U., Hasan, T., Huang, H.-C., & Rizvi, I. (2020). Flow-induced Shear Stress Confers Resistance to Carboplatin in an Adherent Three-Dimensional Model for Ovarian Cancer: A Role for EGFR-Targeted Photoimmunotherapy Informed by Physical Stress. *Journal of Clinical Medicine*, *9*(4), 924. https://doi.org/10.3390/jcm9040924
5. Sorrin, A. J., Ruhi, M. K., Ferlic, N. A., Karimnia, V., Polacheck, W. J., Celli, J. P., Huang, H.-C., & Rizvi, I. (2020). Photodynamic Therapy and the Biophysics of the Tumor Microenvironment. *Photochemistry and Photobiology*, *96*(2), 232–259. https://doi.org/10.1111/php.13209
6. Polacheck, W. J., German, A. E., Mammoto, A., Ingber, D. E., & Kamm, R. D. (2014). Mechanotransduction of fluid stresses governs 3D cell migration. *Proceedings of the National Academy of Sciences*, *111*(7), 2447–2452. https://doi.org/10.1073/pnas.1316848111
7. Polacheck, W. J., & Chen, C. S. (2016). Measuring cell-generated forces: A guide to the available tools. *Nature Methods*, *13*(5), 415–423. https://doi.org/10.1038/nmeth.3834
8. Mathworks. (2020). *The Watershed Transform: Strategies for Image Segmentation*. Retrieved April 30, 2021, from https://www.mathworks.com/company/newsletters/articles/the-watershed-transform-strategies-for-image-segmentation.html

This work was supported in part by the NC Translational and Clinical Sciences Institute (NC TraCS), supported by the Nationa Center for Advancing Translational Sciences (NCATS), National Institutes of Health (NIH)